Available online at www.sciencedirect.com
ScienceDirect
Journal of Hazardous Materials 147 (2007) 205–212
Journal of Hazardous Materials
www.elsevier.com/locate/jhazmat

Phosphate removal from water using lithium intercalated gibbsite

Shan-Li Wang [a,b,*], Chia-Yi Cheng [a], Yu-Min Tzou [a], Ren-Bao Liaw [c], Ta-Wei Chang [d], Jen-Hshuan Chen [a]

[a] *Department of Soil and Environmental Sciences, National Chung Hsing University, Taichung, Taiwan*
[b] *Center of Nanoscience and Nanotechnology, National Chung Hsing University, Taichung, Taiwan*
[c] *Livestock Research Institute, Hsin-Hua, Tainan County, Taiwan*
[d] *Agricultural Engineering Research Center, Jung-Li, Taoyuan County, Taiwan*

Received 2 November 2006; received in revised form 21 December 2006; accepted 22 December 2006
Available online 4 January 2007

Abstract

In this study, lithium intercalated gibbsite (LIG) was investigated for its effectiveness at removing phosphate from water and the mechanisms involved. LIG was prepared through intercalating LiCl into gibbsite giving a structure of $[LiAl_2(OH)_6]^+$ layers with interlayer Cl^- and water. The results of batch adsorption experiments showed that the adsorption isotherms at various pHs exhibited an L-shape and could be fitted well using the Langmuir model. The Langmuir adsorption maximum was determined to be 3.0 mmol g^{-1} at pH 4.5 and decreased with increasing pH. The adsorption of phosphate was mainly through the displacement of the interlayer Cl^- ions in LIG. In conjunction with the anion exchange reaction, the formation of surface complexes or precipitates could also readily occur at lower pH. The adsorption decreased with increasing pH due to decreased $H_2PO_4^-/HPO_4^{2-}$ molar ratio in solution and positive charges on the edge faces of LIG. Anion exchange is a fast reaction and can be completed within minutes; on the contrary, surface complexation is a slow process and requires days to reach equilibrium. At lower pH, the amount of adsorbed phosphate decreased significantly as the ionic strength was increased from 0.01 to 0.1 M. The adsorption at higher pH showed high selectivity toward divalent HPO_4^{2-} ions with an increase in ionic strength having no considerable effect on the phosphate adsorption. These results suggest that LIG may be an effective scavenger for removal of phosphate from water.

Keywords: Gibbsite; Li intercalation; Phosphate; Anion exchange; Ligand exchange; Sorption; Water treatment; ^{31}P MAS NMR; X-ray diffraction

1. Introduction

Phosphorus is an element most commonly associated with eutrophication in surface waters [1–3]. The over-enrichment of lakes, rivers and seas with phosphorus as a result of human activities can accelerate eutrophication that subsequently results in the deterioration of water quality and limits its usage. For example, eutrophication has been linked to shellfish poisoning of humans [4]. The bloom of toxic microalgae species as well as oxygen depletion that results from eutrophication can also have harmful effects on aquatic organisms and can reduce the benthic biomass and biodiversity [2,3,5]. These may further lead to ecological loss and a reduction in the economic values of aquatic ecosystems. Meanwhile, with the growing population of the world, the global fresh water supply is already expected to be limited, so the impact of high levels of phosphorus can ultimately condemn millions of people to an avoidable premature death. Protection of water resources is an urgent task for healthy living and sustainable development. For water conservation, the removal of phosphorus from surface waters and wastewaters to control eutrophication is of great importance.

Conventional techniques for removing phosphorus from waters include physical (e.g., settling and filtration), chemical (e.g., precipitation, ion exchange, and sorption), biological processes (e.g., consumption by algae, bacteria or plants) [6–8]. Among these techniques, anion exchange and adsorption methods are more preferred because of their low cost, ease of equipment use, lower sludge production and the potential of recycling retained phosphorus.

In this study, a novel adsorbent, Li intercalated gibbsite (LIG) was investigated for its effectiveness for phosphate removal from

* Corresponding author at: Department of Soil and Environmental Sciences, National Chung Hsing University, Taichung, Taiwan.
Tel.: +886 4 2284 0373x3406; fax: +886 4 22862043.
E-mail address: slwang@dragon.nchu.edu.tw (S.-L. Wang).

0304-3894/$ – see front matter © 2007 Elsevier B.V. All rights reserved.
doi:10.1016/j.jhazmat.2006.12.067

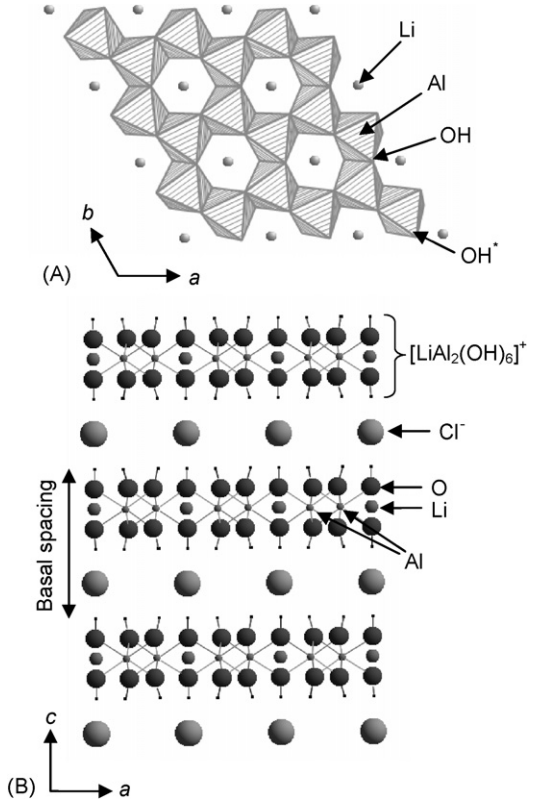

Fig. 1. Crystal structure of lithium intercalated gibbsite projected along the *c* and *b* axes, respectively.

water. This material is synthesized through LiCl intercalation of gibbsite (α-$Al(OH)_3$) or polymorphs and has a chemical formula $[LiAl_2(OH)_6]Cl{\cdot}xH_2O$ [9–12]. Gibbsite has been recognized as an important adsorbent for phosphate in soils and sediments [13–15]. Phosphate ions are adsorbed by gibbsite through ligand exchange of surface OH groups with Al [16–21]. Formation of aluminum phosphate phases on the surface of gibbsite has been previously suggested [21–23]. The reported values for the phosphate adsorption of gibbsite was 0.2 mmol g^{-1} or less, mainly depending on the solution pH and the surface area of gibbsite [14,18,20,24]. After intercalation of lithium salt (e.g., LiCl), the structure of LIG is composed of permanent positive charged $LiAl_2(OH)_6$ sheets with interlayers occupied by counter-anions and H_2O (Fig. 1) [10]. In gibbsite, each of the $Al(OH)_3$ layers consists of nearly close packed OH^- ions in which the Al^{3+} occupy 2/3 of the octahedral holes in the layers [25]. Lithium cations are inserted in the vacant octahedral sites of the gibbsite-like $Al(OH)_3$ layers and contribute the positive charges of the hydroxide layers (Fig. 1A) [10]. The positive charge sites in the hydroxide sheets are counterbalanced by anions intercalating between adjacent hydroxide layers (Fig. 1). Unlike gibbsite whose phosphate ions are only adsorbed on the external surface with pH dependent charges, the internal surface of each individual hydroxide sheet in LIG may additionally serve as adsorbents for phosphate and other anionic contaminants. The adsorption capacity of LIG is therefore expected to be significantly greater than that of gibbsite. Previous studies on the adsorption of some inorganic and organic anions by LIG have demonstrated its reactivity toward these anions [26–29]. For example, a maximum adsorption of 3.81 mmol g^{-1} was previously reported for chromate [29]. To the best of our knowledge, phosphate removal of LIG has not been reported before and has been investigated in this study. The effectiveness of phosphate removal by LIG was studied as a function of pH, ionic strength and adsorbent dosage. X-ray diffraction (XRD) and ^{31}P magic angle spinning nuclear magnetic resonance spectroscopy (^{31}P MAS NMR) were used to study the structures of LIG with and without adsorbed phosphate. This aided the interpretation of the adsorption mechanism of phosphate on LIG.

2. Materials and methods

2.1. Synthesis of LIG

The adsorbent LIG was synthesized through intercalating LiCl into gibbsite (α-$Al(OH)_3$). Ten grams of gibbsite was added into 100 mL 10 M LiCl solution at 90 °C and the temperature of the suspension was maintained at 90 °C for 18 h. Subsequently, the suspension was centrifuged and the collected solids were washed with iced water until free of chloride. Iced water was used to wash the samples to inhibit the Li deintercalation reaction of LIG that would otherwise occur at higher temperatures [28]. The solid product was subsequently dried at 90 °C for 24 h in an oven and stored in a glass vial prior to further use.

2.2. Phosphate adsorption kinetics

Kinetic adsorption of phosphate was observed at pH 4.5 and 9.5. Phosphate solutions were prepared by dissolving NaH_2PO_4 or Na_2HPO_4 into deionized water. The 500 mL of 100 mg L^{-1} phosphate solution at pH 4.5 or 9.5 was added into a 1 L water-jacked reaction vessel and the temperature was adjusted to 25 °C. Then, 0.25 g of the adsorbent was added into the phosphate solution. As a result, the initial phosphate concentration in the suspension was 100 mg L^{-1} while the solids concentration was 0.5 g L^{-1}. This adsorbate/adsorbent ratio was selected to ensure that residual phosphate concentrations were above detectable levels during the experiments. The pH value of the suspension was re-adjusted to a desired value, if necessary, using 10 mM NaOH and HCl solutions, and was maintained constant throughout the experiments. An aliquot of the suspension was extracted at 0, 0.25, 0.5, 0.75, 1, 2, 3, 4.5, 6, 9, 12, 24, 36 and 48 h. The withdrawn samples were filtered through a 0.45-μm cellulose acetate membrane filter to collect the filtrate and adsorbent. The phosphate concentration in the filtrates was determined using the molybdenum blue method [30]. The amount of adsorbed phosphate was calculated using the difference between the initial and final measured phosphate concentrations. The data from the duplicated experiments were then averaged. Meanwhile, the collected adsorbents were washed with deionized water until free of salt, air-dried, and grounded prior to XRD and ^{31}P MAS NMR analyses.

2.3. Phosphate adsorption isotherms

Adsorption experiments were conducted using the batch method. Each experiment was repeated twice. The 20 mg of LIG solids was added into 25 mL phosphate solution, with pH pre-adjusted to 4.5, 6.0, 8.0 or 9.5 using 10 mM HCl and NaOH solutions. The initial phosphate concentrations of the samples at each pH ranged from 0 to 100 mg L^{-1}. Under vigorously stirring the pH value of the suspensions was readjusted to the desired value. The samples were subsequently shaken at 100 rpm at 25 °C for 24 h. The pH values of the samples were measured every 3 h and were readjusted if necessary. After 24 h, the samples were centrifuged at 5000 rpm for 10 min and the pH values of the supernatants were measured. The supernatants were then filtered using 0.45-μm cellulose acetate membrane filters and the phosphate concentrations in the filtrates were measured using the molybdenum blue method [30]. The data of the duplicated analyses were then averaged. The residual sediments of the samples selected for XRD and NMR studies were collected, washed with DI water until free of salt and dried at 110 °C. The samples were then stored in glass vials before use.

The adsorption equilibrium data of phosphate on LIG were analyzed in terms of the Langmuir model. The Langmuir isotherm equation can be rearranged to the linear form given below:

$$\frac{C_e}{x/m} = \frac{C_e}{S_m} + \frac{1}{K_L S_m}$$

where K_L and S_m are Langmuir constants, which are related to the adsorption energy and adsorption maximum, respectively. These constants can be calculated from the slope and intercept of the linear plot with $C_e/(x/m)$ versus C_e, where C_e and x/m are equilibrium concentration and adsorbed phosphate, respectively.

2.4. Effects of adsorbent dosage and ionic strength

The effects of adsorbent dosage and ionic strength on the phosphate removal by LIG were investigated using the batch method. A specific known amount of KH_2PO_4 or K_2HPO_4 was dissolved in 0.001, 0.01 and 0.1 M KCl solutions at pH 4.5 and pH 9.5 to give a 50 mg L^{-1} concentration of phosphate. Subsequently, 25 mL of each phosphate solution was added into a series of centrifuge tubes. To each tube various amounts of LIG were added to make a range of solid concentrations of LIG from 0.1 to 2.5 g L^{-1}. The centrifuge tubes were then mechanically agitated at 100 rpm for 24 h. The pH values of the samples were measured every 3 h and were readjusted if necessary. After 24 h, the samples were centrifuged at 5000 rpm for 10 min. The supernatants were then filtered using 0.45-μm cellulose acetate membrane filters and the residual phosphate concentrations in the filtrates were measured using the molybdenum blue method [30]. The data obtained from the duplicated experiments were then averaged.

2.5. X-ray diffraction and ^{31}P MAS NMR analyses

X-ray diffraction (XRD) patterns of LIG samples were obtained using an X-ray diffractometer (Rigaku Miniflex) with Cu Kα radiation. The XRD patterns were recorded in the range of 2–60° 2θ with a scanning rate of 2° 2θ min^{-1}. The ^{31}P MAS NMR spectra of phosphate-containing LIG samples were collected with a carrier frequency of 201.810 MHz. A 90° pulse was used to excite the spin system and the recycle time was 10 s. The number of collected scans was 1024 for each spectrum. The chemical shift was referenced to the signal of 85% H_3PO_4 solution.

3. Results and discussion

3.1. Adsorption kinetics

The dissociation constants pK_1, pK_2 and pK_3 of H_3PO_4 are 2.15, 7.20 and 12.33, respectively. Depending on the pH value in solution, phosphate ions exist as different ionic species. Therefore, it is necessary to consider the different ionic species while the adsorption reaction is investigated. On the other hand, LIG consists of gibbsite-like layers (Fig. 1). Because the dissolution of gibbsite becomes relatively significant below pH 4 and above pH 10 [31], the LIG structure is also expected to be unstable in the same pH range. To avoid any considerable interference from the dissolution reaction, the phosphate adsorption of LIG was thus investigated in the pH range between 4 and 10.

Fig. 2 shows the adsorption kinetics at pH 4.5 and 9.5, at which $H_2PO_4^-$ and HPO_4^{2-}, respectively, are the primary ions in the solutions. After mixing phosphate solutions with LIG, a fast removal of phosphate from the solutions was observed at either pH. At pH 9.5, the adsorption of HPO_4^{2-} ions reached 1.8 mmol g^{-1} in the first 15 min. This value is equivalent to 3.6 $mmol_c$ g^{-1}, corresponding to 78% AEC of LIG (AEC = 4.6 $mmol_c$ g^{-1}, determined based on the chemical formula of dried LIG). After the first 15 min, the amount of adsorbed phosphate was virtually the same, indicating that

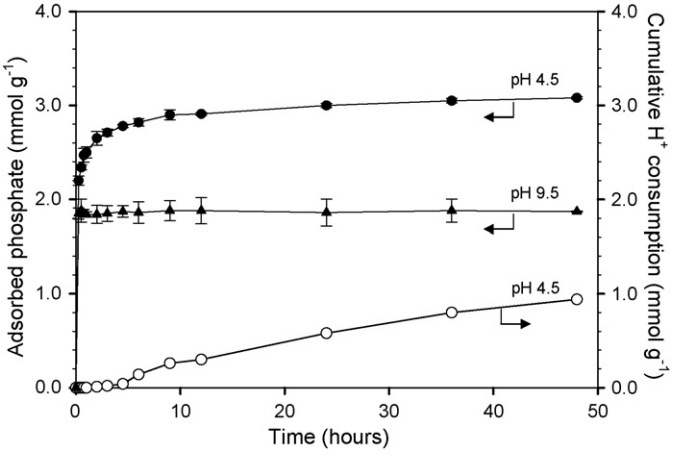

Fig. 2. Phosphate adsorption and cumulative H^+ consumption of lithium intercalated gibbsite at pH 4.5 and 9.5. The initial phosphate concentration was 100 mg L^{-1} while the solids concentration was 0.5 g L^{-1}.

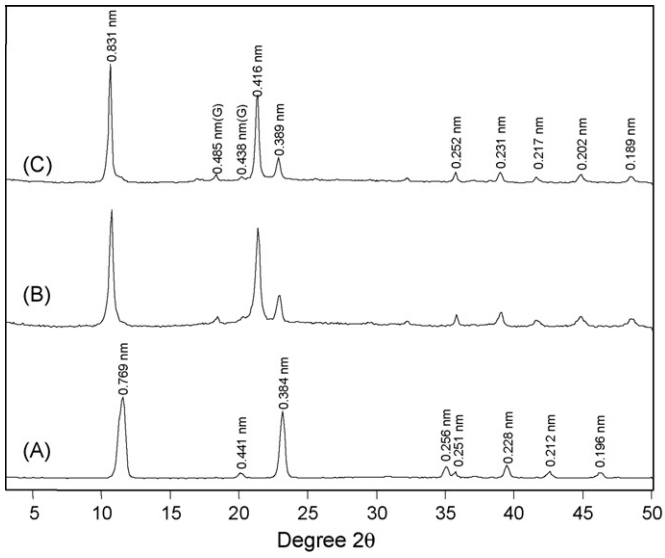

Fig. 3. X-ray diffractions patterns of original LIG (A) and samples collected after phosphate reaction at pH 9.5 (B) and 4.5 (C) for 15 min.

the reaction reached equilibrium within 15 min. Meanwhile, the concurrent monitoring of the solution pH showed no discernible change during phosphate adsorption, implying that the occurrence of ligand exchange of the surface OH groups by phosphate ions was insignificant under this experimental condition. Thus, phosphate ions may be adsorbed primarily through the displacement of the interlayer Cl^- ions in LIG (Fig. 1B). The relative high reaction rate is also characteristic of an anion exchange reaction, in contrast to the slow reaction rate when forming surface complexes or precipitates.

Unlike the reaction at pH 9.5, which attained equilibrium within 15 min, the removal of phosphate at pH 4.5 increased rapidly to 2.2 mmol g^{-1} in the first 15 min and then the increased slowly up to 3.0 mmol g^{-1} after 48 h (Fig. 5). At the same time, addition of HCl solution was required to maintain a constant pH during the reaction (Fig. 2). This result indicates an increasing release of OH^- ions from LIG structure resulting from phosphate adsorption. Ligand exchange of the surface OH groups by $H_2PO_4^-$ ions occurs, consequently resulting in the formation of surface complexes with Al. Since anion exchange is a relatively fast reaction, the portion of removed phosphate involving in slow adsorption is attributed to the formation of surface complexes or precipitates [17,22,23,32]. The time for reaching equilibrium at pH 4.5 is therefore much greater than that at pH 9.5 (Fig. 2).

The XRD patterns of LIG collected after reacting with phosphate at pH 4.5 and 9.5 are shown in Fig. 3. Because the XRD patterns exhibited no change upon increasing reaction time, only the patterns collected at 15 min are shown. Before phosphate adsorption, the basal spacing of LIG containing Cl^- was 0.769 nm (Fig. 3A), which is consistent with the value previously reported [9,10,33]. After reacting with phosphate, the basal spacing of the adsorbent at either pH value shifted to 0.831 nm. The shift of basal spacing indicated the replacement of the interlayer Cl^{-1} ions by phosphate ions. The disappearance of the peak of 0.769 nm in the first 15 min supported the observation revealed

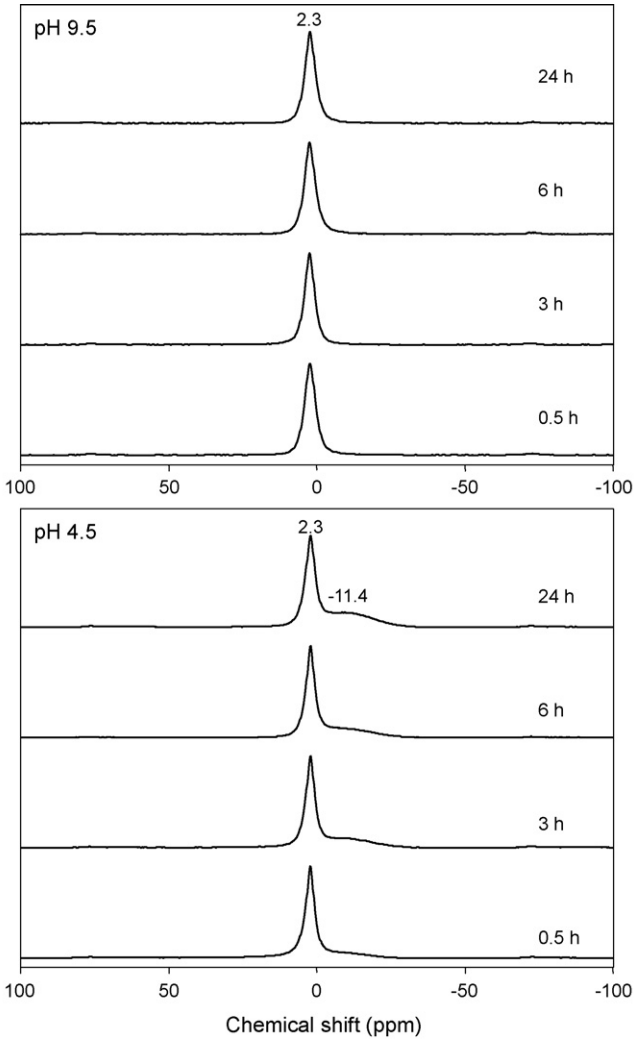

Fig. 4. ^{31}P MAS NMR spectra of LIG reacted with phosphate at pH 9.5 and 4.5 as a function of time.

in Fig. 2 that the anion exchange reaction occurs in the early stage of phosphate adsorption on LIG.

In addition to the reflections of LIG, the reflections appearing at 0.485 and 0.438 nm were contributed by gibbsite (Fig. 3B and C). Since gibbsite was not detected in the original LIG (Fig. 3A), the formation of gibbsite was due to Li deintercalation of LIG. However, the intensities of the reflections of gibbsite were weak and showed no considerable increase upon increasing reaction time. The interference from the formation of gibbsite was therefore not considerable.

Although aluminum phosphate precipitates have the potential to form in the system, the XRD patterns showed no occurrence of crystalline aluminum phosphate, such as variscite ($AlPO_4{\cdot}2H_2O$; $d = 0.304$ nm), metalvariscite ($AlPO_4{\cdot}2H_2O$; $d = 0.476$ nm), wavellite ($Al_3(PO_4)_2(OH)_3{\cdot}5H_2O$; $d = 0.867$ nm) or Na-montebrasite ($NaAlPO_4OH$; $d = 0.297$ nm) [22,23,31,34,35]. To detect adsorbed or amorphous phases, ^{31}P MAS NMR was applied. The ^{31}P MAS NMR spectroscopy is a short-range order tool and therefore can be used to determine the local structure of phosphate in LIG. The results are shown in Fig. 4. A single peak

appeared at 2.3 ppm in the ^{31}P MAS NMR spectra collected for LIG samples at pH 9.5. This peak exhibited a symmetric line shape and showed no changes in its position and line shape upon increasing reaction time (Fig. 4A). On the other hand, this 2.3-ppm peak also appeared predominantly after phosphate adsorption at pH 4.5 for 15 min. Upon increasing reaction time, the peak at 2.3 ppm also showed no change in its position and line shape (Fig. 4B). But, a new peak appeared at −11.4 ppm and its relative intensity increased with increasing reaction time.

The ^{31}P chemical shift of phosphate is determined by the number and type of cations coordinated with phosphate and the bond lengths and angles of phosphate [36,37]. For example, the ^{31}P chemical shifts of aqueous PO_4^{3-}, HPO_4^{2-}, and $H_2PO_4^-$ ions are 8.70, 6.25 and 3.75 ppm, respectively, in relation to H_3PO_4 [38]; the ^{31}P chemical shift decreases as the number of proton bound to phosphate increases. For phosphate bound to Al, the ^{31}P chemical shift will further decrease to more negative values as the number of Al bound to phosphate increases [38,39]. In extreme cases, when four Al atoms are bound to the oxygen atoms of phosphate, such as those in variscite ($AlPO_4{\cdot}2H_2O$), the corresponding ^{31}P chemical shift is −19.2 ppm [40]. Because the ^{31}P chemical shift at 2.3 ppm is between those of $H_2PO_4^-$ (3.75 ppm) and H_3PO_4 (0 ppm), it is assigned to the interlayer phosphate ions involved in H-bonding with the hydroxyl group and interlayer water in LIG. The symmetric line shape of this peak at either pH revealed that the phosphate ions retained in the interlayer of LIG are probably present as a single phase. On the other hand, the broad peak at −11.4 ppm indicates a direct bonding of phosphate with Al and may arise from surface complexes or precipitates of phosphate. The broad width of this peak also indicates a disordered environment of the corresponding phosphate species and the center of this peak is possible a certain weighted mean value for the phosphate of similar chemical species. The curve-fitted result of the ^{31}P MAS NMR spectrum collected at equilibrium showed that the relative intensities of the 2.3- and −11.4-ppm peaks were 66 and 34%, respectively. Using the corresponding adsorbed amount of phosphate (i.e., 3.0 mmol g^{-1}), the concentrations of the corresponding phosphate species were calculated to be 2.0 and 1.0 mmol g^{-1}, respectively. At the same time, the cumulative H^+ consumption in Fig. 2 revealed that the released amount of OH^- due to ligand exchange of $H_2PO_4^-$ was 0.94 mmol g^{-1}. Since the molar ratio of released OH^- and adsorbed $H_2PO_4^-$ was approximately one, adsorbed phosphate may form monodentate complexes on the external surface of LIG at pH 4.5, if surface precipitation was not considered.

Although XRD results showed no indication of the occurrence of crystalline aluminum phosphate phases after phosphate adsorption, the possibility of forming surface precipitates cannot be completely ruled out here. As suggested in Veith and Sposito [22], an amorphous aluminum phosphate with chemical formula $Al(OH)_2H_2PO_4$ was formed after gibbsite interacted with phosphate in the pH range from 2.5 to 9. In this case, two oxygen atoms of phosphate are bound to Al and the other two are terminal OH groups providing a chemical environment of the P atom consistent with the ^{31}P chemical shift at −11.4 ppm. In Lookman et al. [41], the ^{31}P MAS spectrum of aluminum hydroxide reacted with phosphate in 33 mM for 10 days and also showed a broad peak at −11 ppm. This peak was also assigned to amorphous aluminum phosphate on the surface.

The results of kinetic adsorption, XRD and ^{31}P NMR consistently showed that the anion exchange is the main mechanism for phosphate adsorption of LIG at pH 4.5 and 9.5. The interlayer Cl^- ions were replaced by $H_2PO_4^-$ and HPO_4^{2-} ions for the positively charged binding sites in the hydroxide sheets, resulting in the increase in the interlayer spacing (Fig. 3). Meanwhile, the formation of surface complexes or precipitates was also observed at pH 4.5. Previous studies suggested that the OH groups on the basal planes of gibbsite posses no reactivity toward phosphate ions and phosphate adsorption sites are Al atoms situated on the edge faces of the crystal [14,16,17,19,21]. At lower pH, the edges faces carry more positive charges and consequently more significantly attract negatively charged phosphate ions in solution. The positively charged OH groups (e.g., OH^* in Fig. 1A) are also more readily replaced by phosphate ions, which consequently form surface complexes with Al [21,42]. Since LIG consisted of gibbsite-like hydroxide layers (Fig. 1), such a ligand exchange reaction can occur for LIG, as confirmed by the results of kinetic adsorption and ^{31}P MAS NMR. Upon increasing pH, the phosphate adsorption is reduced due to the decrease in positive charges and a build-up of negative charges on the edges of the hydroxide sheets. As a result, formation of surface complexes at pH 9.5 was insignificant and phosphate adsorption dominated by anion exchange reached equilibrium within 15 min.

3.2. Phosphate adsorption at various pHs

Phosphate adsorption isotherms at pH 4.5, 6.0, 8.0 and 9.5 are shown in Fig. 5. Regardless of the pH and phosphate composition in the solutions, all isotherms exhibit the L-shape, suggesting that limited sites are available for phosphate adsorption. As more sites are occupied by phosphate ions, it becomes increasingly difficult for the subsequent phosphate ions to be adsorbed on the remaining vacant sites. The adsorption isotherms were analyzed

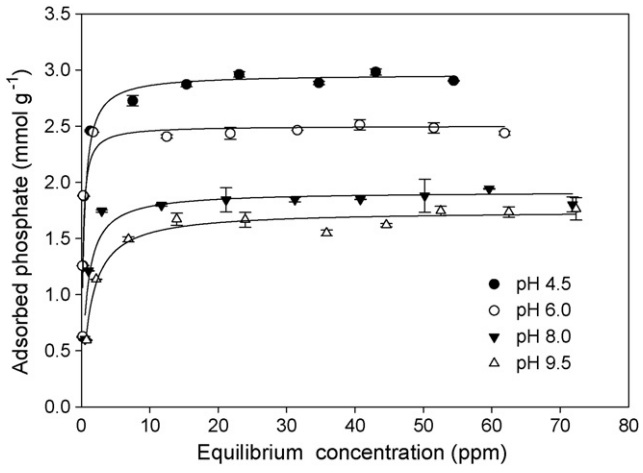

Fig. 5. Phosphate adsorption isotherms of LIG at various pHs.

Table 1
Langmuir adsorption maximum (S_m) and adsorption energy (K_L) for phosphate adsorption on lithium intercalated gibbsite at various pHs

pH	S_{max} (mmol g^{-1})	K_L	r^2
4.5	3.0	2.6	0.9996
6.0	2.5	5.8	0.9997
8.0	1.9	2.1	0.9978
9.5	1.8	0.6	0.9964

in terms of the Langmuir model to give the fitted constants listed in Table 1. The adsorption maximum S_m was 3.0 mmol g^{-1} at pH 4.5 and decreased to 1.8 mmol g^{-1} as the pH value was increased to 9.5 (Table 1).

XRD patterns of the adsorbent collected at different pHs are shown in Fig. 6. After interacting with $H_2PO_4^-$ at pH 4.5 for 24 h, the basal spacing shifted to 0.831 nm (Fig. 6). The XRD patterns of the adsorbents exhibited no discernible changes as the pH was increased up to 9.5. Especially, the basal spacing was also 0.831 nm for LIG interacting with HPO_4^{2-} at pH 9.5 (Fig. 6). No change in the basal spacings for the interlayer $H_2PO_4^-$ and HPO_4^- due to their similar sizes and interactions with the hydroxide layers of LIG.

Fig. 7 shows the ^{31}P MAS NMR spectra of LIG collected after phosphate adsorption for 24 h at various pHs. At pH 4.5, a sharp peak at 2.3 ppm and a broad shoulder centered at −11.4 ppm were seen. The relative intensity of the peak at −11.4 gradually decreased with increasing pH and was undetectable at pH 9.5. Only one single peak at 2.3 was shown in the ^{31}P MAS NMR spectrum for the sample interacting with HPO_4^{2-} at pH 9.5 for 24 h (Figs. 4 and 7). The ^{31}P chemical shift of 2.3 ppm was assigned to phosphate ions retained in the interlayer of LIG. As the reaction pH was increased, there was no change in the position of the 2.3-ppm peak showing that the interactions of $H_2PO_4^-$ and HPO_4^{2-} ions with the hydroxide layers are similar, as confirmed by the same corresponding basal spacings (Fig. 6). Meanwhile, with increasing pH, the decrease in the relative intensity of the peak at −11.4 ppm indicated a decrease in the formation of surface complexes or precipitates.

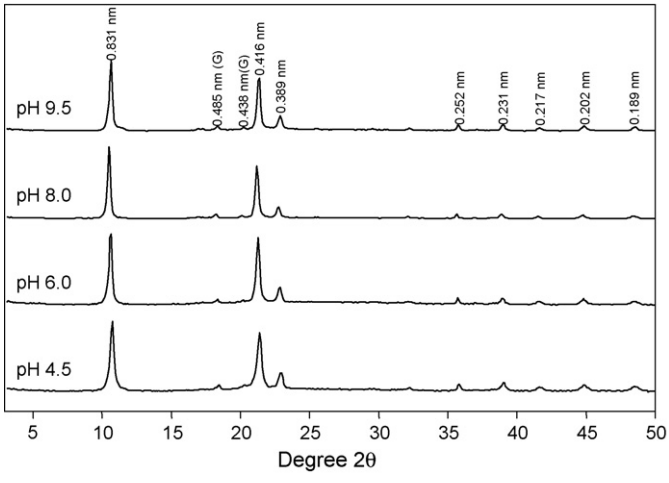

Fig. 6. X-ray diffraction patterns of LIG collected after reacting with phosphate solutions at pH 4.5, 6.0, 8.0 and 9.5 for 24 h.

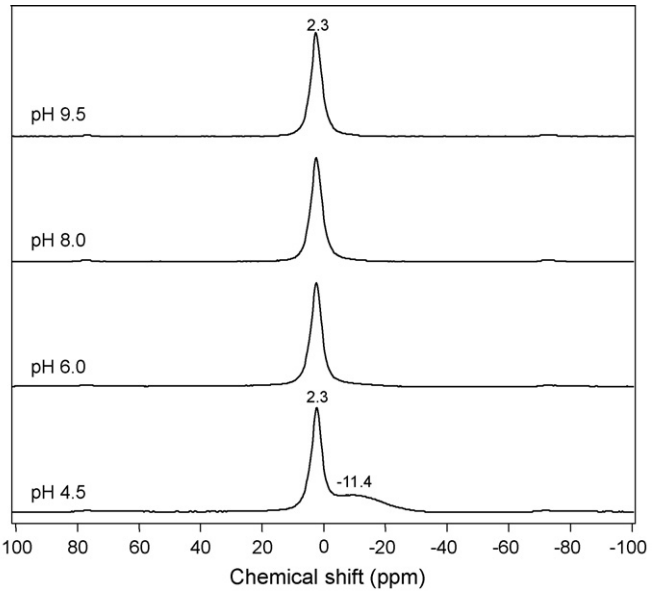

Fig. 7. The ^{31}P MAS NMR spectra of LIG collected after reacting with phosphate solutions at pH 4.5, 6.0, 8.0 and 9.5 for 24 h.

As revealed from the results of kinetic adsorption, phosphate ions were adsorbed on LIG mainly through replacing the interlayer Cl^- ions. Because the amount of positively charged sites contributed by Li^+ in the hydroxide sheets is independent of pH, the decrease in the corresponding phosphate adsorption upon increasing pH results from the decrease in the $H_2PO_4^-/HPO_4^{2-}$ molar ratio. To exchange each Cl^- ion, one $H_2PO_4^-$ ion or 0.5 HPO_4^{2-} ion was adsorbed. From pH 4.5 to 9.5, the molar ratio of monovalent $H_2PO_4^-$ ions to divalent HPO_4^{2-} ions in solution decreases. Therefore, the amount of adsorbed phosphate decreased with increasing pH. On the other hand, the formation of surface complexes or precipitates is concurrent and become significant at lower pH, as revealed by the decrease in the relative intensity of the ^{31}P chemical shift of −11.4 ppm. Upon increasing pH, the decrease in positive charges and build-up of negative charges on the edges of the hydroxide sheets also result in a decrease in phosphate adsorption. As a result, formation of surface complexes is insignificant at pH 9.5 and anion exchange is the predominant mechanism for phosphate adsorption.

3.3. Effects of adsorbent dosage and ionic strength

The effects of adsorbent dosage and ionic strength on phosphate removal at pH 4.5 and 9.5 are presented in Fig. 8. With 50 mg L^{-1} phosphate in 0.001 M KCl, the removal rate increased with increasing adsorbent dosage. At pH 9.5, an adsorbent dosage of 1.20 g L^{-1} produced 94.2% removal of phosphate (Fig. 8A). The removal rate further increased to 99.2 and 99.9% when the dosage was increased to 1.50 and 2.00 gL^{-1}, respectively. The extent of phosphate removal in 0.001 M, 0.01 M and 0.1 M KCl solutions was similar at the different adsorbent dosages. For example, with 1.5 g L^{-1} adsorbent dosage, the removal rates were 99.2, 98.7 and 96.3% in 0.001, 0.01 and 0.1 M KCl, respectively. When the adsorbent dosage was increased to

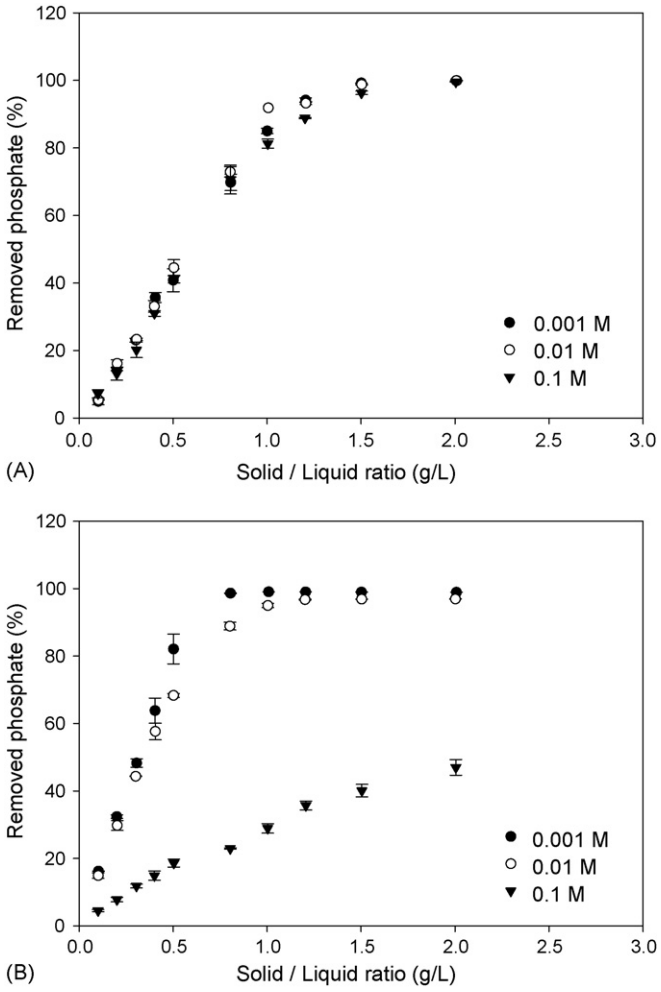

Fig. 8. Effects of adsorbent dosage and ionic strength on the removal rate of phosphate by LIG at pH 9.5 (A) and 4.5 (B). The initial phosphate concentration was 50 mg L^{-1}.

2.00 g L^{-1}, the removal rates in the different concentrations of KCl were all above 99.5%.

At pH 4.5 the removal rate was 98.6% when using 0.80 g L^{-1} adsorbent to treat 50 mg L^{-1} phosphate in 0.001 M KCl. The removal rate increased above 99% as the dosage was increased to 1.00 g L^{-1} or more. The adsorbent dosage required for achieving a 99% removal rate was lower at pH 4.5 than pH 9.5. Meanwhile, the effect of increasing ionic strength on phosphate removal was more significant at pH 4.5, compared with the result at pH 9.5. For example, with 0.80 g L^{-1} adsorbent, the removal rates were 98.6% in 0.001 M KCl, 88.9% in 0.01 M KCl and 22.9% in 0.1 M KCl. The removal rate significantly decreased as the ionic strength was increased to 0.1 M KCl (Fig. 8). Even using 2.0 g L^{-1} adsorbent, the maximum removal rate of phosphate in 0.1 M KCl was 47.0%. It is clear that phosphate adsorption was more strongly inhibited at pH 4.5 than pH 9.5 with increasing ionic strength. This is mainly due to the higher affinity of LIG toward anions with higher charge density, with divalent HPO_4^{2-} ions adsorbed more preferentially than monovalent $H_2PO_4^-$ ions. In other words, the background Cl^- ions affect the adsorption of $H_2PO_4^-$ ions more strongly than HPO_4^{2-} ions.

4. Conclusions

Phosphate adsorption on LIG proceeded mainly through the anion exchange of the interlayer Cl^- ions by phosphate ions. Anion exchange was relatively rapid and could be completed within minutes. With decreasing pH, the formation of surface complexes or precipitates became relatively significant; Coulombic attraction could readily occur at lower pH in conjunction with anion exchange reaction. The slow reaction rate of the forming surface complexes resulted in a longer equilibrium time at lower pH. Ionic strength showed no considerable effect on the adsorption of divalent HPO_4^{2-} ions. On the other hand, a significant decrease in the removal rate occurred for monovalent $H_2PO_4^-$ ions as the ionic strength was increased to 0.1 M. The results indicated that LIG can be used as an effective scavenger for removing phosphate from waters.

Acknowledgement

The authors are grateful to the National Science Council, Taiwan for financial support (NSC 93-2313-B-005-055, 94-2313-B-005-065, and 95-2313-B-005-018).

References

[1] E.M. Bennett, S.R. Carpenter, N.F. Caraco, Human impact on erodable phosphorus and eutrophication: a global perspective, Bioscience 51 (2001) 227.
[2] D.M. Anderson, P.M. Glibert, J.M. Burkholder, Harmful algal blooms and eutrophication: nutrient sources, composition, and consequences, Estuaries 25 (2002) 704.
[3] V.H. Smith, Eutrophication of freshwater and coastal marine ecosystems—a global problem, Environ. Sci. Pollut. Res. 10 (2003) 126.
[4] M.M. Brett, Food poisoning associated with biotoxins in fish and shellfish, Curr. Opin. Infect. Dis. 16 (2003) 461.
[5] J.H. Landsberg, The effects of harmful algal blooms on aquatic organisms, Rev. Fish. Sci. 10 (2002) 113.
[6] L.E. de-Bashan, Y. Bashan, Recent advances in removing phosphorus from wastewater and its future use as fertilizer (1997–2003), Water Res. 38 (2004) 4222.
[7] G.K. Morse, S.W. Brett, J.A. Guy, J.N. Lester, Review: phosphorus removal and recovery technologies, Sci. Total Environ. 212 (1998) 69.
[8] D.W. de Haas, M.C. Wentzel, G.A. Ekama, The use of simultaneous chemical precipitation in modified activated sludge systems exhibiting biological excess phosphate removal. Part 1. Literature review, Water SA 26 (2000) 439.
[9] V.P. Isupov, L.E. Chupakhina, V.V. Boldyrev, Synthesis of intercalation compounds of aluminum hydroxide with lithium salts, Dokl. Chem. 332 (1993) 206.
[10] A.V. Besserguenev, A.M. Fogg, R.J. Francis, S.J. Price, D. O'Hare, Synthesis and structure of the gibbsite intercalation compounds $[LiAl_2(OH)_6]X$ $\{X = Cl,Br,NO_3\}$ and $[LiAl_2(OH)_6Cl_2H_2O$ using synchrotron X-ray and neutron powder diffraction, Chem. Mater. 9 (1997) 241.
[11] A.M. Fogg, D. O'Hare, Study of the intercalation of lithium salt in gibbsite using time-resolved in situ X-ray diffraction, Chem. Mater. 11 (1999) 1771.
[12] J. He, M. Wei, B. Li, Y. Kang, D.G. Evans, X. Duan, Preparation of layered double hydroxides, Struct. Bond. 119 (2006) 89.
[13] E.O. McLean, Chemistry of soil aluminum, Commun. Soil Sci. Plant Anal. 7 (1976) 619.
[14] R.L. Parfitt, Anion adsorption by soils and soil minerals, Adv. Agron. 30 (1978) 1.

[15] J. Kopacek, J. Borovec, J. Hejzlar, K.U. Ulrich, S.A. Norton, A. Amirbahman, Aluminum control of phosphorus sorption by lake sediments, Environ. Sci. Technol. 39 (2005) 8784.
[16] D. Muljadi, A.M. Posner, J.P. Quirk, The mechanism of phosphate adsorption by kaolinite, gibbsite, and pseudoboehmite.Part II. The location of the adsorption sites, J. Soil Sci. 17 (1966) 230.
[17] J.H. Kyle, A.M. Posner, J.P. Quirk, Kinetics of isotopic exchange of phosphate adsorbed on gibbsite, J. Soil Sci. 26 (1975) 32.
[18] S.S.S. Rajan, Changes in net surface charge of hydrous alumina with phosphate adsorption, Nature 262 (1976) 45.
[19] R.L. Parfitt, A.R. Fraser, J.D. Russell, V.C. Farmer, Adsorption on hydrous oxides. II. Oxalate, benzoate and phosphate on gibbsite, J. Soil Sci. 28 (1977) 40.
[20] L. Lijklema, Interaction of orthophosphate with iron (III) and aluminum hydroxides, Environ. Sci. Technol. 14 (1980) 537.
[21] S. Goldberg, J.A. Davis, J.D. Hem, The surface chemistry of aluminum oxides and hydroxides, in: G. Sposito (Ed.), The Environmental Chemistry of Aluminum, Lewis Publishers, New York, 1996, pp. 271–331.
[22] J.A. Veith, G. Sposito, Reactions of aluminosilicates, aluminum hydrous oxides, and aluminum oxide with o-phosphate: The formation of X-ray amorphous analogs of variscite and montebrasite, Soil Sci. Soc. Am. J. 41 (1977) 870.
[23] W.H. van Riemsdijk, F.A. Weststrate, G.H. Bolt, Evidence for a new aluminum phosphate phase from reaction rate of phosphate with aluminum hydroxide, Nature 257 (1975) 473.
[24] D. Muljadi, A.M. Posner, J.P. Quirk, The mechanism of phosphate adsorption by kaolinite, gibbsite, and pseudoboehmite Part I. The isotherms and the effect of pH on adsorption, J. Soil Sci. 17 (1966) 212.
[25] H. Saalfeld, M. Wedde, Refinement of the crystal structure of gibbsite, $Al(OH)_3$, Z. Krist. 139 (1974) 129.
[26] A.M. Fogg, J.S. Dunn, S.G. Shyu, D.R. Cary, D. O'Hare, Selective ion-exchange intercalation of isomeric dicarboxylate anions into the layered double hydroxide$[LiAl_2(OH)_6]ClH_2O$, Chem. Mater. 10 (1998) 351.
[27] A.M. Fogg, V.M. Green, H.G. Harvey, D. O'Hare, New separation science using shape-selective ion exchange intercalation chemistry, Adv. Mater. 11 (1999) 1466.
[28] S.L. Wang, R.J. Hseu, R.R. Chang, P.N. Chiang, J.H. Chen, Y.M. Tzou, Adsorption and thermal desorption of Cr(VI) on Li/Al layered double hydroxide, Colloid. Surf. A 277 (2006) 8.
[29] L.C. Hsu, S.L. Wang, Y.M. Tzou, C. Lin, J.H. Chen, The removal and recovery of Cr(VI) by Li/Al layered double hydroxide (LDH), J. Hazard. Mater. 142 (2007) 242–249.
[30] S.R. Olsen, L.E. Sommers, Phosphorus, in: A.L. Page, R.H. Miller, D.R. Keeney (Eds.), Methods of Soil Analysis. Part 2. Chemical and Microbiological Properties, Soil Science Society of America, Madison, Wisconsin, USA, 1982, pp. 403–430.
[31] W.L. Lindsay, P.M. Walthall, The solubility of aluminum in soils, in: G. Sposito (Ed.), The Environmental Chemistry of Aluminum, Lewis Publishers, New York, 1996, pp. 333–361.
[32] S.S.S. Rajan, K.W. Perrott, W.M.H. Saunders, Identification of phosphate-reactive sites of hydrous alumina from proton consumption during phosphate adsorption at constant pH values, J. Soil Sci. 25 (1974) 428.
[33] X. Hou, D.L. Bish, S.L. Wang, C.T. Johnston, R.J. Kirkpatrick, Hydration, expansion, structure, and dynamics of layered double hydroxides, Am. Miner. 88 (2003) 167.
[34] T. Goldshmid, A.J. Rubin, Determination of soluble species and precipitates of aluminum phosphate, Sep. Sci. Technol. 23 (1988) 2269.
[35] W.L. Lindsay, P.L.G. Vlek, S.H. Chien, Phosphate minerals, in: J.B. Dixon, S.B. Weed (Eds.), Minerals in Soil Environment, Soil Science Society of America, Madison, 1989, pp. 1089–1130.
[36] J.J. Fitzgerald, S.M. DePaul, Solid state NMR spectroscopy of inorganic materials: an overview, in: J.J. Fitzgerald (Ed.), Solid-State NMR Spectroscopy of Inorganic Materials, American Chemical Society, Washington, DC, 1999, pp. 1–133.
[37] U. Sternberg, F. Pietrowski, W. Priess, The influence of structure and coordination on the P-31 chemical shift in phosphates, Z. Physik. Chem. Neue Fol. 168 (1990) 115.
[38] R.F. Mortlock, A.T. Bell, C.J. Badke, ^{31}P and ^{27}Al NMR investigations of highly acidic, aqueous solutions containing aluminum and phosphorus, J. Phys. Chem. 97 (1993) 767.
[39] I.L. Mudrakovskii, V.P. Shmachkova, N.S. Kotsarenko, V.M. Mastikhin, Investigation of aluminum phosphates by high-resolution ^{27}Al and ^{31}P NMR in the solid phase, Kinet. Catal. 32 (1991) 1085.
[40] W.F. Bleam, P.E. Pfeffer, J.S. Frye, ^{31}P solid-state nuclear magnetic resonance spectroscopy of aluminum phosphate minerals, Phys. Chem. Miner. 16 (1989) 455.
[41] R. Lookman, P. Grobet, R. Merckx, K. Vlassak, Phosphate sorption by synthetic amorphous aluminum hydroxide: a ^{27}Al and ^{31}P solid-state MAS NMR spectroscopy study, Eur. J. Soil Sci. 45 (1994) 37.
[42] W. Stumm, Coordinative interactions between soil solids and water—an aquatic chemist's point of view, Geoderma 38 (1986) 19.